

# The Tunnel Source n-MOSFET: A Novel Asymmetric Device for Low Power Applications

Venkatagirish N.<sup>1</sup>, Ahmet Tura<sup>1</sup>, Ritesh Jhaveri<sup>1</sup>, Hsu-Yu Chang<sup>1</sup> and Jason Woo<sup>1</sup>

<sup>1</sup>Department of Electrical Engineering, University of California, Los Angeles, CA 90095, USA

Phone: +1-(310) 206 3279 E-mail: woo@ee.ucla.edu

## 1. Introduction

As MOSFETs are aggressively scaled, their performance is severely limited by short channel effects (DIBL and  $V_{TH}$  roll-off), off-state and gate leakages, parasitic capacitances and resistances, etc. These, in addition to  $V_{DD}$  scaling limitation and high sub-threshold swing ( $>60\text{mV/dec}$ ) give rise to high  $I_{OFF}$  and make power dissipation an enormous challenge, especially for low power/low current applications. New device innovations are essential to achieve low  $I_{OFF}$  and high  $g_m$  with high  $R_{OUT}$  for digital and analog applications, respectively. Tunnel FETs (TFETs) [1-2] can potentially achieve sub-60mV/dec subthreshold swing (SS) and operate at lower  $V_{DD}$ , since source injection is dictated by band-to-band tunneling instead of diffusion. Most TFETs suffer from  $I_{ON}$  degradation and high average SS close to  $V_{TH}$ . To overcome these problems, we have proposed the Tunnel Source (PNPN) n-MOSFET [3], as shown in Fig. 1. This novel asymmetric device has the potential for steep sub-threshold behavior, improved  $I_{ON}/I_{OFF}$ , high  $R_{OUT}$  and gain ( $g_m \times R_{OUT}$ ) at low bias currents. It also possesses excellent immunity against short channel effects which improves scalability into sub-50nm regime and makes it an attractive candidate for low power digital and analog operations.

## 2. Concept of Tunnel Source (PNPN) n-FET

The proposed nFET as shown in Fig. 1 has a  $p^+$  source and the current is controlled by band-to-band tunneling between the source and the channel, which is governed by the Fermi selection rule, the tunneling barrier height ( $\phi_{TUN}$ ) and width ( $W_{TUN}$ ) [3]. The band diagram for the tunnel FET in the OFF-state and the ON-state are shown in Fig. 2 (a) and (b) respectively. To reduce the tunnel junction resistance, a smaller bandgap source material (SiGe) has been proposed previously to lower  $\phi_{TUN}$  [4]. However, it is also necessary to reduce  $W_{TUN}$ . In our proposed structure, the thin fully depleted  $n^+$  layer increases the lateral electric field and therefore reduces  $W_{TUN}$ , minimizing the potential drop across the tunneling junction and therefore improving  $I_{ON}$ . The sub-threshold swing is minimized when the pocket is *just* fully depleted as shown in band diagram or when the tunneling distance is just equal to the pocket width.

## 3. Device Performance

Fig. 3 shows the comparison between the I-V characteristics for a Tunnel Source (PNPN) n-MOSFET and corresponding conventional SOI MOSFET with the same structural parameters ( $L_G=90\text{nm}$ ,  $T_{OX}=25\text{\AA}$ ,  $T_{SI}=60\text{nm}$  at the same  $I_{OFF} = 10\text{pA}/\mu\text{m}$ . Pocket width=4nm, Pocket doping= $5 \times 10^{19}\text{cm}^{-3}$ ). The simulations have been performed with ATLAS device simulator, calibrated with experimental data obtained from silicon tunnel diodes [3]. With a narrow ( $\sim 4\text{nm}$ )  $n^+$  region, the PNPN n-MOSFET shows a steep sub-threshold behavior (SS $\sim 30\text{mV/dec}$  over 3-4 decades at 300K) with low  $I_{OFF}$ . This is highly beneficial for low standby power applications.

Fig. 4 shows the behavior of subthreshold swing vs.  $V_{GT}$ . It is seen that for the tunnel FET with pocket width 4nm the swing goes below the diffusion limit of 60mV/dec for a wide range. The  $n^+$ -pocket has to be just fully depleted, which is crucial for beneficial device operation. For a wider pocket with the same doping, the pocket is partially depleted; therefore the device is diffusion limited and behaves like a conventional SOI MOSFET (Fig. 4). The band diagrams shown in Fig. 5 (a) - fully depleted pocket and Fig. 5 (b) - partially depleted pocket, show this clearly. Thus, fully depleted  $n^+$  layer is essential for the device to achieve steep sub-threshold behavior and high  $I_{ON}$ .

Excellent robustness to SCEs provided by the PNPN n-MOSFET can be seen in Fig. 6 where the DIBL and  $V_T$  roll-off are reduced as the channel length decreases. This is due to negligible source-to-channel coupling and reduced influence of drain bias on the source tunneling junction. This is particularly favorable for low standby power where the  $I_{ON}/I_{OFF}$  ratio as well as low  $I_{OFF}$  is maintained with scaling to sub-50nm gate lengths.

The tunneling injection mechanism, negligible DIBL and improved resistance to SCEs of the PNPN n-MOSFET have favorable implications for low operating power (low  $I_{BIAS}$ ) analog applications as well. Fig. 7 shows that the transconductance ( $g_m$ ) of the Tunnel Source n-MOSFET for a just-fully depleted pocket width of 4nm is higher as compared to the conventional SOI device, at low  $I_{BIAS}$  ( $V_D = 0.8\text{V}$ ), due to the tunneling injection mechanism at the source. ( $g_{mSAT}$  is still lower than the conventional SOI).

Fig. 8 shows that the PNPN n-MOSFET exhibits an improvement in  $R_{OUT}$  over the conventional SOI for the given channel length. This can be attributed again to reduced drain coupling (DIBL) and resistance to SCEs. When channel length decreases the  $R_{OUT}$  is governed by DIBL, rather than channel length modulation. As a result, the intrinsic gain ( $g_m \times R_{OUT}$ ) of the PNPN n-MOSFET is also higher than the conventional device, especially at low bias currents, as shown in Fig. 9.

## 4. Conclusions

The novel Tunnel Source (PNPN) n-MOSFET is highly promising for stand-by power reduction as it can decrease the subthreshold swing and  $I_{OFF}$  beyond the limits for conventional devices. It also shows excellent short channel immunity, significantly higher  $g_m$ ,  $R_{OUT}$  and intrinsic gain in addition to good high frequency characteristics, especially at low  $I_{BIAS}$ .

## Acknowledgements

The authors would like to acknowledge and thank DARPA for providing funding for the project.

## References

- [1] T. Krishnamohan, et al, p. 947 (2008).
- [2] F. Mayer et al, *IEDM*, p. 163 (2008)
- [3] Venkatagirish N. et al, *TED* Vol. 55, No. 4, p. 1013 (2008)
- [4] K. K. Bhuvalka, et al, *TED*, Vol. 52, No. 7, p. 1541 (2005)

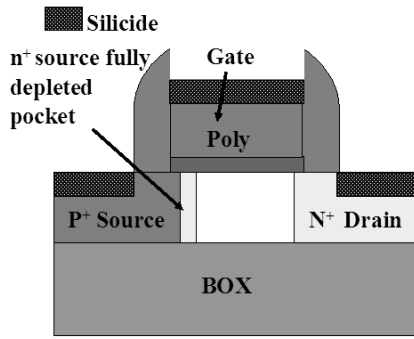


Fig. 1 Device structure of the tunnel source (PNPN) n-FET

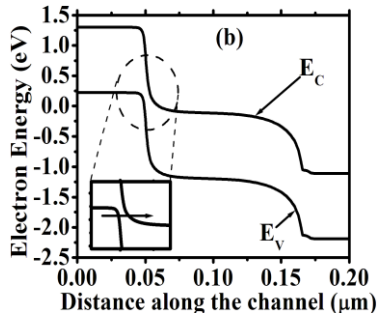
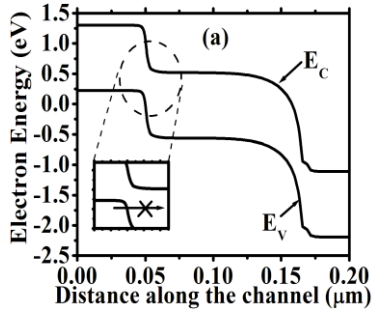


Fig. 2 Band Diagram of the tunnel n-FET in the (a) OFF state and (b) ON state

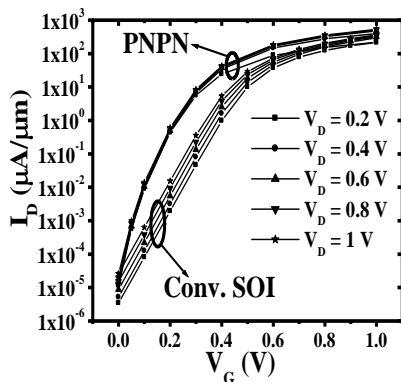


Fig. 3 Comparison of  $I_D$ - $V_G$  curves for the PNPn tunnel FET and Conventional SOI MOSFET. The tunnel FET shows  $<60\text{mV/dec}$  subthreshold swing

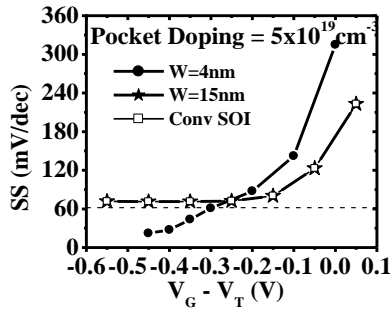


Fig. 4 SS vs  $V_{GT}$  for the tunnel n-FET with 2 widths and conv. SOI n-FET. When  $W = 4\text{nm}$  (fully depleted) the SS goes below  $60\text{mV/dec}$

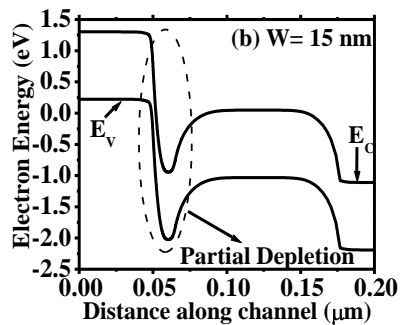
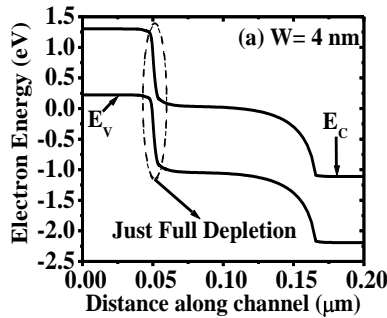


Fig. 5 Band diagram when the pocket is (a) fully depleted and (b) partially depleted

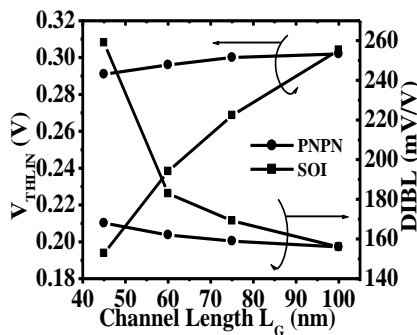


Fig. 6 Scaling of the tunnel n-FET with respect to  $V_{Th}$  roll off and DIBL

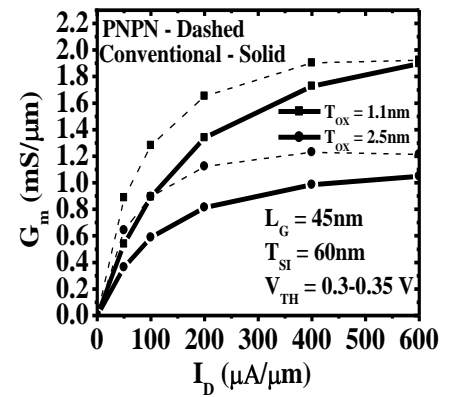


Fig. 7 Transconductance of the PNPn tunnel FET in comparison to conv. SOI n-FET. The tunnel n-FET has higher transconductance due to tunneling injection mechanism

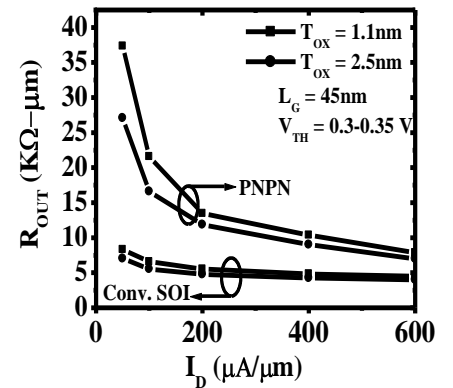


Fig. 8 Comparison of output resistance of the PNPn tunnel FET and conv. SOI n-FET

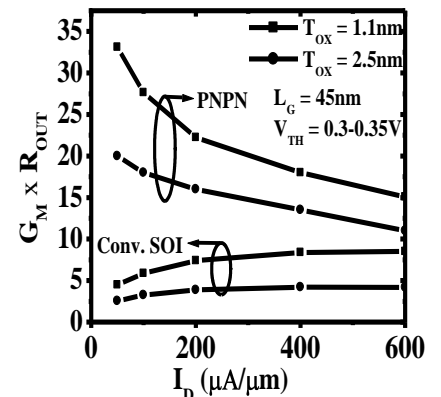


Fig. 9 Comparison of the intrinsic gain of the PNPn tunnel FET and the conv. SOI n-FET. The tunnel n-FET has higher gain performance.